https://doi.org/10.5194/egusphere-2024-3227
Preprint. Discussion started: 21 October 2024

Intraseasonal variability of North Pacific Intermediate Water induced by mesoscale eddies

Ren Qiang[1, 2], Yansong Liu[1, 2], Feng Nan[1, 2, 3], Ran Wang[1, 2], Xinyuan Diao[1, 2, 3], Fei Yu[1, 2, 3]*, Zifei Chen[1, 2]*, Jianfeng Wang[1, 2], Xinchuang Liu[1, 2]

[1] Key Laboratory of Ocean Observation and Forecasting, Institute of Oceanology, Chinese Academy of Sciences, Qingdao, China
[2] Key Laboratory of Ocean Circulation and Waves Institute of Oceanology, Chinese Academy of Sciences, Qingdao, China
[3] College of Marine Sciences, University of Chinese Academy of Sciences, Qingdao 266071, China

Corresponding authors: Fei Yu (yuf@qdio.ac.cn) and Zifei Chen (chenzifei@qdio.ac.cn)

https://doi.org/10.5194/egusphere-2024-3227
Preprint. Discussion started: 21 October 2024

Abstract:
The North Pacific Intermediate Water (NPIW) is one of the most crucial water masses in the global ocean, significantly impacting physical, biological, chemical, and ecological processes. The challenges inherent in direct continuous observation of NPIW have been limiting the understanding of its short-term variability. Utilizing 14 months of data from three moorings (146°E, 25°N, M1; 122.6°E, 22.3°N, M2; 126°E, 18°N, M3), this study reveals the characteristics of the NPIW and its consistent intraseasonal variability from 60 to days across a range of latitudes and spatiotemporal scales. Direct measurement show depth variations at 700 m, 600 m, and 550 m for M1, M2, and M3, respectively. The analysis reveals a significant association between NPIW variation and mesoscale eddies, evidenced by lead-lag coefficients of 0.6, 0.5, and 0.55 for SLA and salinity at M1, M2, and M3. During anticyclonic (cyclonic) eddies, a positive (negative) SLA corresponds to relatively warm (cooler) and saline (fresh) characteristics of NPIW. Further analysis has shown that due to the inverse S-shaped structure of salinity in the North Pacific region, the vertical movement of water masses within mesoscale eddies leads to inverse phase changes between the NPIW and deeper water. Also the circulation and water masses near the western boundary are relatively complex, mesoscale eddies also induce mixing of the surrounding water masses and thus modify the NPIW properties. The result found that under the influence of the eddy, the change in salinity in the intermediate layer can reach to 0.3 psu, and the depth of the low-salt core can vary by hundreds of meters. Therefor studying the variability of NPIW is crucial for accurately predicting mesoscale eddy transport of heat and energy to ocean's intermediate layer, and understanding its response to climate change, its role in the global carbon cycle, and its impact on marine ecosystems.

Index Terms and Keywords
Intraseasonal variation of 60-80 days in the North Pacific intermediate water.
Anticyclonic (cyclonic) eddies induced warm (cooler) and saline (fresh) of NPIW.
Vertical and horizontal transport of eddies affects the NPIW

plain-language summary
North Pacific Intermediate Water (NPIW), is one of the most crucial water masses in the global ocean, however, current studies of their variability have focused on seasonal, interannual, or interdecadal scales, while studies of shorter-term variability are scarce due to observational difficulties. Using direct measurement data from three moorings, it reveals the intraseasonal variability of NPIW with a periods of 60-80 days at different regions. It was found that the intraseasonal variation of NPIW is mainly caused by mesoscale eddies, further studies show that anticyclonic (cyclonic) eddies induced a positive (negative) SLA corresponds to relatively warm (cooler) and saline (fresh) characteristics of NPIW. In addition, processes such as the upward and downward movement of internal water masses caused by mesoscale eddies and the resulting changes in local water masses and circulation can jointly influence changes in the NPIW.

https://doi.org/10.5194/egusphere-2024-3227
Preprint. Discussion started: 21 October 2024

Understanding these dynamics is critical for assessing the NPIW's response to climate change and its implications for the global carbon cycle and marine ecosystems.

Introduction

The North Pacific Intermediate Water (NPIW) is a pivotal component of the North Pacific's water mass and extensively studied due to its significant role in climate dynamics and oceanic processes. This water mass, forming in the northwestern subtropical gyre, specifically in the mixed region between the Kuroshio Extension and Oyashio front, is characterized by its low salinity and relatively cooler temperatures at depths of approximately 400 to 1200 meters, also its density is centered around 26.8 σ_θ. (Talley, 1993, 1995; Yasuda et al., 1997; You et al., 2003; Masujima et al., 2009). The distribution and transport pathways of NPIW have been a focal point of oceanographic research, many studies have shown that the NPIW is widely distributed in the North Pacific Ocean, and that it is transported by complex water masses and circulation (Qiu, 1995; Ueno & Yasuda, 2004; You, 2003; Yasuda, 2004; Fujii et al., 2013; Gordon and Fine, 1996; Kashino et al., 1996; Kashino et al., 1999).
Moreover, the NPIW is an important intermediate water mass connecting the upper and deeper layers of the ocean, and furthermore its intra-seasonal scale of variability is one of the most important links between high-frequency variability and medium- to long-term cyclic variability, and the variability it produces has important implications for physical, biological, chemical, and ecological processes such as dissolved oxygen, nutrient distribution, and thermohaline transport (Nishioka et al., 2020; Talley et al., 1993; Hansell et al., 2002; Auad et al., 2003; Tsunogai et al., 2002; Ohkushi et al., 2003). Nishioka et al. (2020) highlight the critical role of NPIW in global carbon cycle by connecting nutrients between deep and surface waters, particularly emphasizing the nutrient enrichment in the subarctic Pacific. Talley (1993) describes the formation of NPIW in the northwestern subtropical gyre and its modification, which affects salinity and oxygen levels. Hansell et al. (2002) discuss the export of dissolved organic carbon (DOC) with NPIW formation, indicating significant biogeochemical implications. Auad et al. (2003) examine the response of NPIW to climate warming, showing how changes in atmospheric forcing can alter its properties. NPIW also plays an important role in global biogeochemical fluxes such as carbon and nutrient cycling (Tsunogai et al., 2002; Ohkushi et al., 2003).
Since NPIW is one of the most important water masses in the global ocean, most of studies focus on its seasonal, interannual or interdecadal variations in different regions, and these variability is largely influenced by multi-scale ocean-atmosphere interactions (Masuda et al., 2003; Ohshima et al., 2010; Bingham& Lukas., 1995; Solomon et al., 2003; Qiu et al., 2011; Van et al., 1993). The seasonal cycles of water mass properties in the North Pacific subtropical gyre were delved into, emphasizing distinct seasonal patterns and their implications (Bingham & Lukas, 1995). Using a four-dimensional variational data assimilation system, Masuda et al. (2003) highlighted the seasonal state of the NPIW. Further investigations focused on the inflow and outflow variations

https://doi.org/10.5194/egusphere-2024-3227
Preprint. Discussion started: 21 October 2024

between the Okhotsk Sea and the Pacific during winter seasons, revealing the complexity of seasonal exchanges (Ohshima et al., 2010).In studies of longer time scale variations, the significant interannual and decadal variabilities of the NPIW linked to large-scale wind forcing is revealed by Nakano et al. (2005). Additionally, Wong et al. (1999) and Oka et al. (2017) also report freshening of the NPIW. Also, Wang et al. (2016) revealed that the semiannual variability of water masses at the northern and southern hemispheric convergence near 8° N. It was found that the NPIW exhibits positive (negative) salinity anomalies corresponding to an intense (weakened) and zonally elongated (contracted) Kuroshio Extension (KE) jet, suggesting a close relationship between oceanic currents and salinity patterns (Qiu et al., 2011). Salinity decreases in the density surface above the NPIW salinity minimum and increases in the density surface below the salinity minimum were observed, based on hydrographic observations in the subtropical gyre of the North Pacific from the 1980s and 1990s to the 2000s, indicating changes in the ocean's salinity structure over time (Kouketsu et al., 2007).

However, the majority of the studies mentioned above focus on time scales exceeding a few hundred days, and also the NPIW are located in the deep layers below the subsurface, where direct and long-term observations are difficult. More than that, there is often a large bias in the salinity representation of the water masses in the intermediate layer of the model data, there are very few studies of less than 100-day scale variations in the NPIW. In a localized area along the western boundary, Mensah et al. (2015) examines the intraseasonal to seasonal variability of intermediate water east of Luzon and Taiwan by hydrographic data from several cruises, and this study mainly focuses on the influences of different water masses on the intermediate water east of Taiwan and the transport variations of Kuroshio Intermediate Water. Ren et al. (2022) found an intraseasonal variability of the intermediate water mass of ~80 days from direct observations of the subsurface moorings east of Taiwan, and that this variability is associated with mesoscale eddies. The research areas of these studies are only concentrated in very small local areas, which is insufficient to demonstrate the widespread and persistent existence of NPIW's variability characteristics of less than 100 days.

Mesoscale eddies are rotating eddies that are widely found in the oceans, with survival periods ranging from a few days to several hundreds of days, and radii of up to several hundreds of kilometers (Wyrtki et al., 1976; Richardson, 1983; Robinson, 1985; Chelton et al., 2007; Chelton et al., 2011; Zhang et al., 2014; Wunsch et al., 2007; Martínez-Moreno et al., 2021). Currently, there have been many studies on mesoscale eddies, which have a clearer understanding of their generation mechanisms and characteristics (Meredith et al., 2012; Frenger et al., 2013; Chelton., 2013; Busecke et al., 2019; Wunsch &Ferrari, 2004; Qiu et al., 2005; Dong et al., 2014; Chaigneau et al., 2008;Chaigneau et al., 2009). Some studies have shown that mesoscale eddies can affect depths of up to thousands of meters, and in some cases even thousands of meters of the seafloor (Zhang et al., 2015; Thoppil et al., 2011; Zhang et al., 2016; Zhang et al., 2015; George et al., 2021; Waite et al., 2016; Hausmann et al., 2017). Within the range of NPIW generation, propagation and distribution, there is also a high incidence

https://doi.org/10.5194/egusphere-2024-3227
Preprint. Discussion started: 21 October 2024

of mesoscale eddies, and the depth at which NPIW is located is not consistent at different latitudes. It is therefore of great interest to investigate whether mesoscale eddies, as a nexus affecting ocean dynamical energy transport at depths of up to several kilometers, have an impact on the NPIW in different regions and with different thermohaline characteristics.

Nakanowatari et al. (2015) pointed out that there are currently many shortcomings in relying on model data to study the characteristics and distribution of NPIW due to the lack of observational data support. In this study, we utilize a long time series of high-resolution observations of the NPIW from three subsurface mooring deployed at different spatial and temporal scales in the North Pacific Ocean to study the intraseasonal variability of the NPIW, is essential for understanding the intricate relationship between ocean processes, climate change and marine ecosystems.

Data and Methods

1. Mooring data

To study the variation of North Pacific Intermediate Water (NPIW), we deployed three mooring systems in the Northwest Pacific region, as shown in Fig. 1. The locations, observation periods, and equipment setups of these three moorings, M1, M2, and M3, are described as follows. The mooring M1 is located at 146°E and 25°N, with an observation period from April 2017 to June 2018; M2 is located to the east of Taiwan on the western boundary, at 122.67°E and 22.3°N, with an observation period from August 2019 to December 2020; while M3 is located at 126°E and 18°N, with an observation period from January 2016 to June 2017. All three moorings were equipped with conductivity-temperature-depth measuring instruments (CTD, with type of Sea-Bird Electronics SBE 37) at intervals of 100 m between depths of 400 and 1000 m. All CTD setups were set to sample every 10 minutes. The data used in this paper were processed for daily averages after deleted the abnormal value and smoothed with a 7-day running mean to remove high frequency variations.

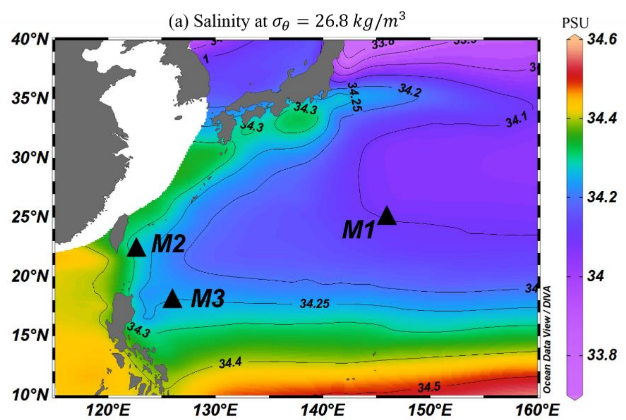

https://doi.org/10.5194/egusphere-2024-3227
Preprint. Discussion started: 21 October 2024

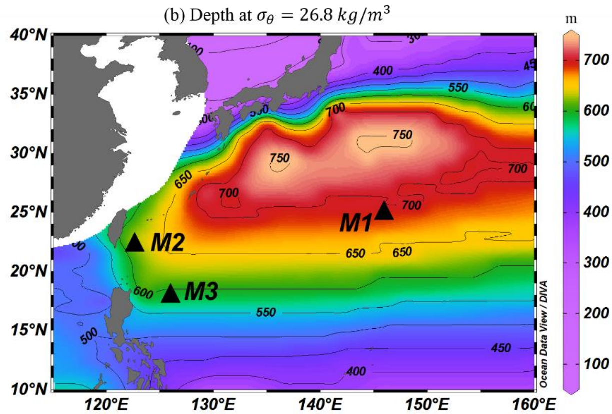

Figure 1. Distribution of salinity (a) and depth (b) along the $26.8\sigma_\theta$ isopycnic at Northwestern Pacific. The color shading and black line in (a) and (b) represent the salinity and depth, respectively. The black triangle is the mooring location: Mooring 1 (M1), Mooring 2 (M2) and Mooring 3 (M3). Salinity and depth in the Fig. 1 are taken from climatological averaged data from World Ocean Atlas 13, and plot with *Ocean Data View.*

2. World Ocean Atlas 2013

In order to see the distribution of NPIW in the Northwest Pacific, we chose the WOA13 data. The WOA13 V2 produced by NOAA's National Oceanographic Data Center - Ocean Climate Laboratory (The data available online at: https://www.ncei.noaa.gov/products/world-ocean-atlas), which contains processed climate field data including in situ temperature, salinity, dissolved oxygen, apparent oxygen utilisation (AOU), percent oxygen saturation, phosphate, silicate and nitrate (Boyer et al., 2013). These data are annual, seasonal and monthly synoptic periods at standard depths of the global ocean at a data resolution of 1°.

3. The Copernicus Marine Environment Monitoring Service (CMEMS) data.

In this article, we utilized satellite altimetry product data to track changes in sea surface height and geostrophic current fields. The data used comes from the Archiving, Validation and Interpretation of Satellite Oceanographic data (AVISO), provided by The Copernicus Marine Environment Monitoring Service (CMEMS, (http://www.marine.copernicus.eu). AVISO's data and products are employed not only in ocean applications but also in hydrology, coastal areas, glaciology, and other fields. The resolution of the sea surface height anomaly and current field data used in this article is 1/4°, covering the observation periods of three sets of subsurface moorings. Furthermore, to analyze changes in temperature and salinity around the subsurface moorings, we also utilized the Multi Observation Global Ocean 3D Temperature Salinity Height Geostrophic Current and Mixed Layer Depth (MLD) data product provided by CMEMS. This data source integrates in-situ observations and satellite observations globally. The time span of this data product extends from January 1993 to

https://doi.org/10.5194/egusphere-2024-3227
Preprint. Discussion started: 21 October 2024

the present, with a time resolution of weekly or monthly. It provides global Level-4 (L4) analyses of ocean 3D temperature, salinity, geopotential height and geostrophic current, which vertical direction from surface to 5500-m depth is divided into 33 layers, as well as 2D Mixed Layer Depth (MLD) on a 1/4° regular grid. This study has been conducted using E.U. Copernicus Marine Service Information; insert all relevant DOIs links here: https://doi.org/10.48670/moi-00145; https://doi.org/10.48670/moi-00149;

Result

The time series of NPIW from different mooring site

It has been shown that NPIW can be widely distributed within the North Pacific Ocean (Talley, 1993, 1995; Yasuda et al., 1997; You, 2003; Qiu, 1995), and follows a dynamically consistent path through the eastern subtropical gyre to the Indonesian Throughflow (Gordon and Fine, 1996; Kashino et al., 1996; Kashino et al., 1999; Fujii et al., 2013). Further research revealed that NPIW circulation is related to diapycnal-meridional overturning generated around the Okhotsk Sea, contributing to the cross-gyre transport from the subarctic to subtropical gyres (Yasuda, 2004). The physical processes that determine the density range of NPIW (σθ = 26.7–26.9) were examined, finding that the salinity/depth characteristic and the transport mechanism of NPIW are impacted by regional precipitation over evaporation in the upper-layer subarctic North Pacific (Qiu, 1995). More than that, the NPIW can carry by Mindanao Current to western equatorial pacific (Bingham and Lukas, 1994). Based on the results of previous studies, in this study, we determined the approximate distribution of the NPIW from the WOA13 showed in Fig. 1, and our subsurface observations are effective in capturing changes in the NPIW

To gain an initial understanding of the NPIW characteristics at the locations of our three deployed moorings, we employed the WOA database to create decadal average maps of salinity and depth distribution on the 26.8σ_θ isopycnal, as illustrated in Fig. 1. The NPIW shows significant local variability, with the NPIW showing lower salinity values and its core depth of approximately 34.1 psu and 700 m near M1 mooring site, respectively. As NPIW disperses southward and westward, the minimum salinity of NPIW is increases and its depth becomes shallower. Near the M2 mooring location, the low salinity value and depth adjust to about 34.25 psu and 600 meters, respectively. M3 near 18°N, which can be seen in Fig. 1 to be located close to the edge of the NPIW distribution, has a salinity minimum value close to that at M2, but the depth of the low-salinity core becomes further shallower to ~550 metres. Thus, the moorings utilized in this study have effectively observed NPIW, capturing its significant spatial and temporal variability across different regions.

Observations from the M1 mooring over more than a year, as shown in Fig. 2a, reveal that the low salinity core of the NPIW has an average depth of approximately 700 meters, fluctuating within the isopycnal range of 26.4-27σ_θ, with the minimum salinity

https://doi.org/10.5194/egusphere-2024-3227
Preprint. Discussion started: 21 October 2024

value being around 34.15 psu. The observed salinity minima at M1 were also found to be slightly higher compared to the climatological averaged data showed in Fig. 1a. Additionally, significant temporal variations in salinity were observed at depths of 400-900 meters by the M1 mooring. Although the changes in the minimum salinity values of NPIW's core layer at approximately 600-800 meters were relatively minor, significant fluctuations still occurred at the boundaries of the low salinity core and its depth. The M2 mooring located east of Taiwan near the western boundary, observed salinity below 400 meters as depicted in Fig. 2c. The low salinity core varied between the isopycnals of 26.6-26.8 σ_θ, showing more significant changes than those observed at M1, with average minimum salinity values and depths of approximately 34.2 psu and 600 meters, respectively, which are higher than the minimum salinity values observed at the M1 location. And it is interesting to note that the low-salt core of M2 exhibits discontinuities, such as the salinity measured in April-May 2020 in Fig. 2c, which is close to 33.6 psu, splitting the low-salt core with a salinity value of around 34.2 psu. At the more southerly M3 mooring, as illustrated in Fig. 2e, the low salinity core also displayed a discontinuous distribution, with seven significant low salinity events observed over a year. The average minimum salinity value between the isopycnals of 26.6-26.8 σ_θ was 34.3 psu, with corresponding temperatures and depths of approximately 8°C and 550 meters, respectively. A distinctive feature of M3 was that the depth of the NPIW's low salinity core was shallower than that at M1 and M2, and the minimum salinity was significantly higher than M1 and M2. The results of NPIW observed by the three differently positioned subsurface mooring are basically consistent with the spatial distribution characteristics of NPIW in the North Pacific Ocean in the WOA data.

Upon comparing Fig. 2a, 2c, and 2e, it appears that the intermediate water masses at the M2 location exhibit greater variability, while those at the M1 location show relatively weaker variations. From the corresponding salinity standard deviation plots (Fig. 2b, 2d, and 2f), it is observed that the M1 mooring displays the smallest standard deviation at the NPIW core depth of approximately 700 meters, indicating higher stability in intermediate layer salinity. Conversely, the salinity at the levels of NPIW for M2 and M3 shows greater variability. The largest standard deviation in salinity at the mooring M2 is 0.7 psu at around 600 meters, shown in Fig. 2d, while a significant standard deviation in salinity around 0.3 psu is observed between 500-600 meters fro mooring M3. This variability in salinity in intermediate layer is also depicted in the T-S (Temperature-Salinity) plot in Fig. 3, where the range of salinity changes at the mooring M2 is the largest among the three observed locations, ranging from 34.13 psu to 34.35 psu, with M1 showing the smallest variation. Differences in standard deviations also illustrate the variability of NPIW changes across regional locations, with the least variability at 25°N, possibly related to its deeper depth. The greater variability in intermediate layer salinity near the M2 location may be associated with complex local circulations and water masses, where the influence of Kuroshio Intermediate Water (KIW) and South China Sea Intermediate Water (SCSIW) under the effect of the Kuroshio or eddies significantly impacts the area (Menash et al., 2015; Ren et al., 2022).

https://doi.org/10.5194/egusphere-2024-3227
Preprint. Discussion started: 21 October 2024

In addition to previous observations, an analysis of Fig. 2a, 2c, and 2e reveals a consistent feature observed in the NPIW is that its salinity variations largely coincide with the fluctuations of the isopycnal. For instance, during the period between May and June 2017 as depicted in Fig. 2a, an increase in salinity was noted at times when the isopycnal were concave downward, suggesting that the low salinity core tended to be shift to deeper depths. Conversely, during periods when the isopycnal were convex upward the overall salinity contours tended to rise as shown between July and September 2017 in Fig. 2a,, resulting in a shallower depth of the low salinity core. These observations suggest that the variations in NPIW may be governed by a unified mechanism that correlates salinity changes with the vertical displacement of isopycnal.

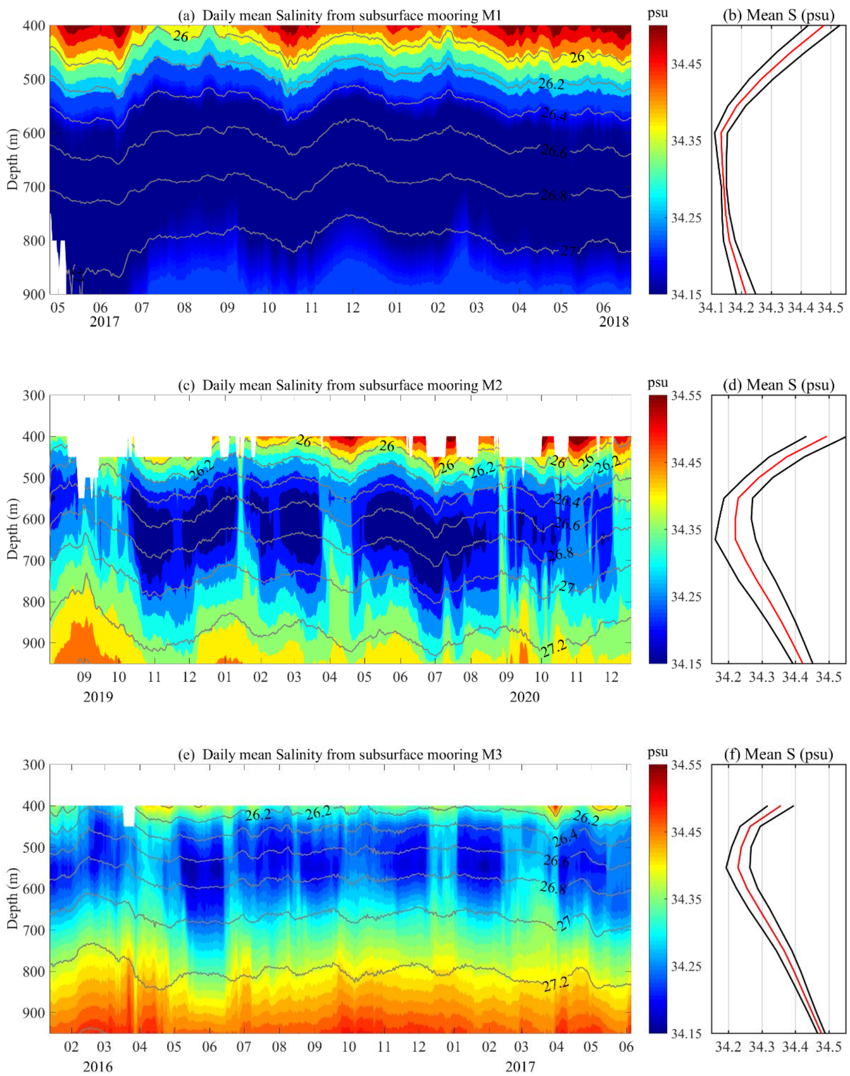

Figure 2. The observation of salinity from subsurface mooring. (a), (c) and (e)

https://doi.org/10.5194/egusphere-2024-3227
Preprint. Discussion started: 21 October 2024

represent time series plots of salinity measured at different observation times for the three moorings, respectively. M1 is observed from April 2017-June 2018, M2 is observed from August 2019-December 2020 and M3 is observed from January 2016-June 2017. Color shading and the gray lines represent the salinity and isopycnic in (a), (c) and (e),, respectively. In (b), (d) and (f), the red line and black line represent the mean salinity and standard deviation of salinity over the observation period, respectively.

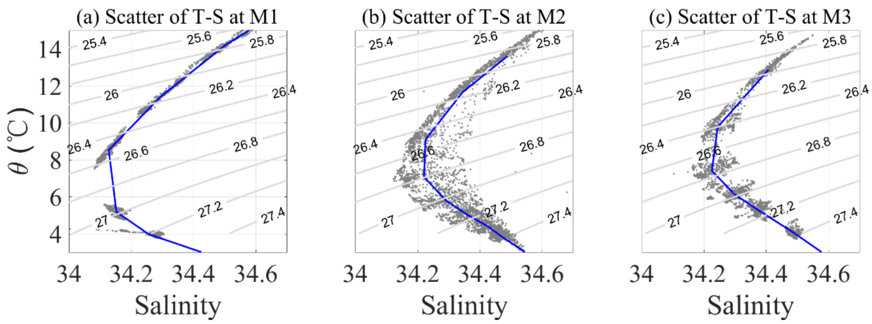

Figure 3. The Temperature-Salinity plot from M1 (a), M2 (b) and M3 (c). The gray line represents the isopycnic, and the bule line represent the average T-S curve at the observation time.

Intraseasonal variations of NPIW

From the analysis of salinity time series in the previous section, discontinuous characteristics of intermediate layer low salinity changes were identified, manifesting as increases or decreases of salinity corresponding to the vertical fluctuations of isopycnal. To understand the potential periodicity of these low salinity variations at intermediate layer, we applied spectral analysis methods, specifically conducting wavelet analyses on the intermediate layer salinity measurement by the three moorings. The NPIW is defined as a water mass with salinity between 34.0 ~ 34.3 psu and depth between 300 ~ 800 m according to You et al. (2003) and Tally et al. (1993), combined with Fig. 2, we take the depth of the intermediate water mass at M1 as 500-800 m within the isopycnals of 26.2-26.7 σ_θ in this study. The wavelet analysis results of the salinity averaged over 500-800 m at the M1 showed in Fig. 4a-b indicate an intraseasonal variability periods of ~70-80 days. However, this intraseasonal variation cycle exhibits temporal variability, it was more significant from May 2017 to April 2018, while the signal strength of the cycle significantly decreased after April 2018. Fig. 4c-d represent the results of the wavelet analysis of averaged salinity at 500 m to 700 m at M2, with a similar ~80 days period as on the M1 result, the intraseasonal signals at M2 also exhibit variability during different observation periods. The period from the beginning of the observations in September 2019 to August 2020 seems to have a much larger range of variability, with Fig. 4c showing ~80 days of variability, whereas the period around 60 days from September 2020 onwards becomes relatively faster. The observation results

https://doi.org/10.5194/egusphere-2024-3227
Preprint. Discussion started: 21 October 2024

from mooring M3 averaged salinity at 450 m to 650 ma s shown in Fig. 4e-f, indicate relatively stable intraseasonal variation periods of 70-80 days throughout the observation period.

To more clearly observe the periodic variations in salinity, we calculated the anomalies of the salinity at each depth for each mooring during the observation period and used a 40-100 day band-pass filter. Fig. 5a shows that intraseasonal signals are present across the 400-900 m depth range for the M1 mooring, and we can clearly see the weakening of these signals after April 2018, consistent with the wavelet analysis results from Fig. 4a. However, the filtering results also indicate significant differences in the strength of the intraseasonal signals at different depths, with stronger signals above 700 m and weaker signals below 700 m. Interestingly, there is an inverse correlation across the 700 m boundary on the M1 mooring, where positive anomalies in salinity between 500-700 m coincide with negative anomalies between 700-900 m.

The band-pass filtering results for the M2 mooring also showed the strongest intraseasonal signal at the 700 m layer, with inverse phase changes observable after May 2020, while the strongest signals from March to May 2020 exhibited consistent changes throughout the all depth. For the M3 mooring, the strongest intraseasonal signals were found around 550 m, corresponding to the core of the NPIW's low salinity. The intra-seasonal variability signal significantly weakened below 750 m. Additionally in Fig. 5c, the larger intraseasonal signals are observed during two periods: April to July 2016 and January to April 2017, with weaker intraseasonal signals from August to December 2016, as reflected in the wavelet spectrum in Fig. 4e.

Combining the wavelet analysis and the corresponding band-pass filtering results from the three moorings reveals that within the extensive distribution range of the NPIW in the Western Pacific, observations across different times and locations consistently indicate a typical intraseasonal variation in the NPIW.

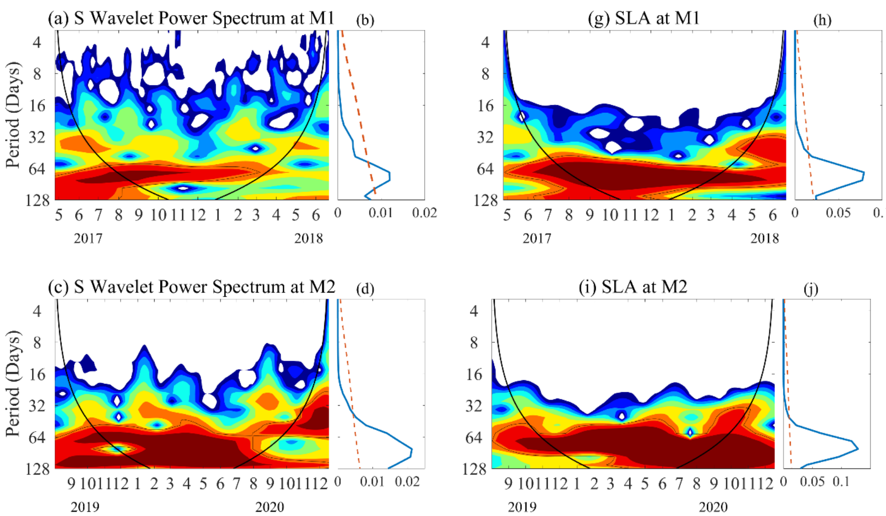

https://doi.org/10.5194/egusphere-2024-3227
Preprint. Discussion started: 21 October 2024

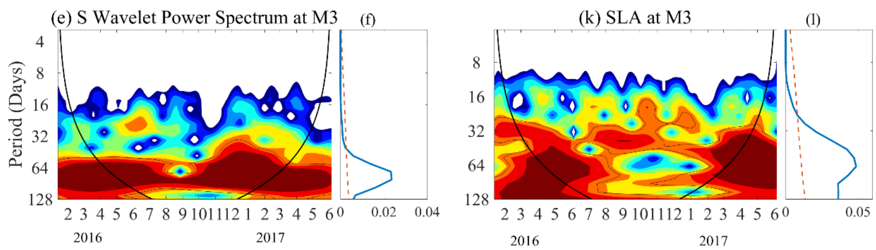

Figure 4. The wavelet power spectrum for salinity from 500 to 800 m at M1, from 500 to 700 m at M2 and from 500-700 m at M3 in (a), (c) and (e), respectively. (b), (d) and (f) are the corresponding global spectrum of salinity in (a), (c) and (e), where the red dashed line denotes the 95% confidence level. (g), (i) and (k) are the wavelet power spectrum for Sea Level Anomaly at the mooring site M1, M2 and M3, also the (h), (j) and (l) are the corresponding global spectrum of SLA. The thick black line represent 95% confidence level in Fig. 4.

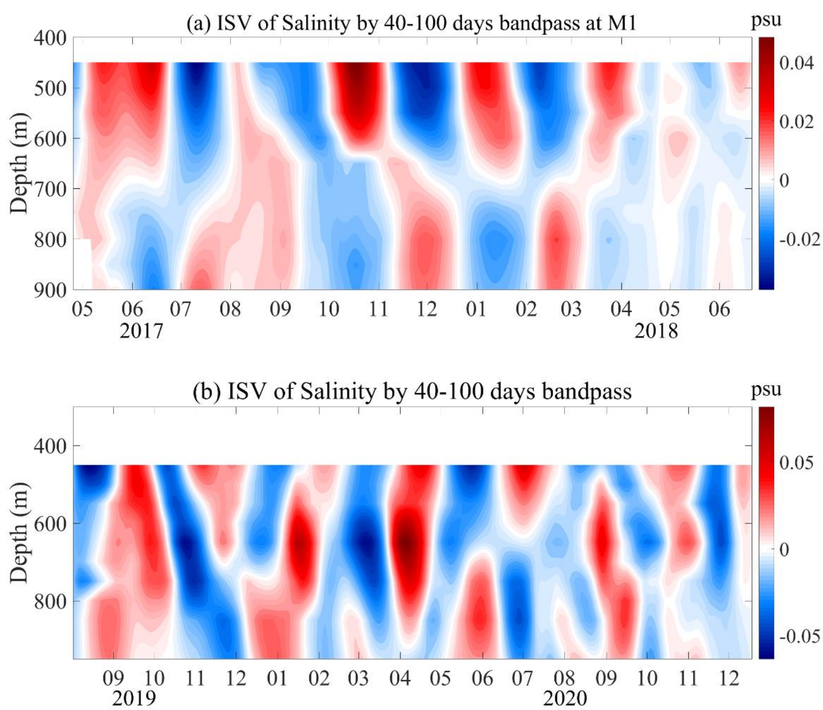

https://doi.org/10.5194/egusphere-2024-3227
Preprint. Discussion started: 21 October 2024

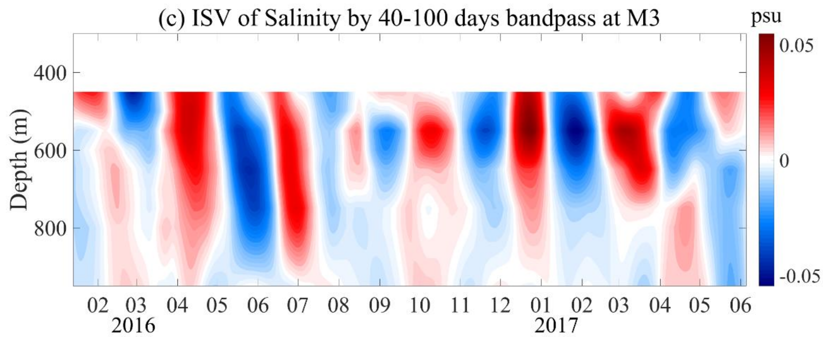

Figure 5. The salinity anomalies by 40-100 days bandpass at M1, M2 and M3.

Disscussion

Relationship between salinity and SLAs

The previous study has clearly demonstrated significant intraseasonal variations in the intermediate layer at different regions. Next, we analyze the potential sources of these intraseasonal signals. Typically, in oceanic, the intraseasonal variations are primarily associated with wind fields and eddies. In our study areas, mesoscale eddies are one of the most typical features, and especially in the western boundary region is a high activity of eddies. To ascertain the presence of similar periodic variations, we initially conducted wavelet analysis on the Sea Level Anomalies (SLAs) at the three mooring locations, derived from satellite altimetry. The results, depicted in Fig. 4g to 4l, reveal a 60-80 days period in the SLA across mooring locations M1 to M3. This period aligns closely with the salinity variation cycles measured by the moorings, indicating a strong correlation between SLA and salinity variations in this region.

To further clarify their relationship, we analyzed the average temperature and salinity at intermediate layer after applying a 20-120 day band-pass filter to discuss the potential correlation between the SLA and these parameters, with the results presented in Fig. 6. At the M1 mooring location, we observed that the SLA was predominantly positive during the observation period, with correlation coefficients of 0.55 and 0.45 with temperature and salinity, respectively. Although these correlation coefficients are not exceptionally high, it is still noticeable that higher temperatures and salinities correspond to periods of positive SLA, whereas negative SLA tend to coincide with lower temperatures and salinities in the intermediate layer. This pattern is further supported by the T-S diagram at M1 shown in Fig. 7a, where water characteristics of relatively lower temperature and salinity (or higher temperature and salinity)

https://doi.org/10.5194/egusphere-2024-3227
Preprint. Discussion started: 21 October 2024

correspond to negative (or positive) SLA. For the mooring M2, Fig. 6b shows correlation coefficients of 0.4 and 0.3 between SLA and temperature and salinity, respectively, indicating a slightly weaker correlation compared to M1. Nonetheless, both Fig. 6b and Fig. 7b demonstrate a positive correlation between SLA and temperature-salinity variables. At the mooring M3, temperature-salinity variations and their correlation with SLA are weaker during the observation period, with lower correlation coefficients. However, similar to M1 and M2, Fig. 6c and Fig. 7c show that periods with significant negative SLA, such as between April-May 2017, correspond to relatively lower salinity and temperature, with salinity values reaching as low as 34.2 psu. Conversely, periods of significant positive SLA, such as between April 2016 and May-June 2017 at M3, correspond to higher temperature and salinity, with salinity reaching up to 34.3 psu. These findings in Fig. 6 and Fig. 7 indicate that moments of significant temperature-salinity variability across the NPIW distribution can be associated with positive (or negative) SLAs regardless of location and time, suggesting that there is a relationship between temperature and salinity characteristics at intermediate layer and sea surface height anomalies.

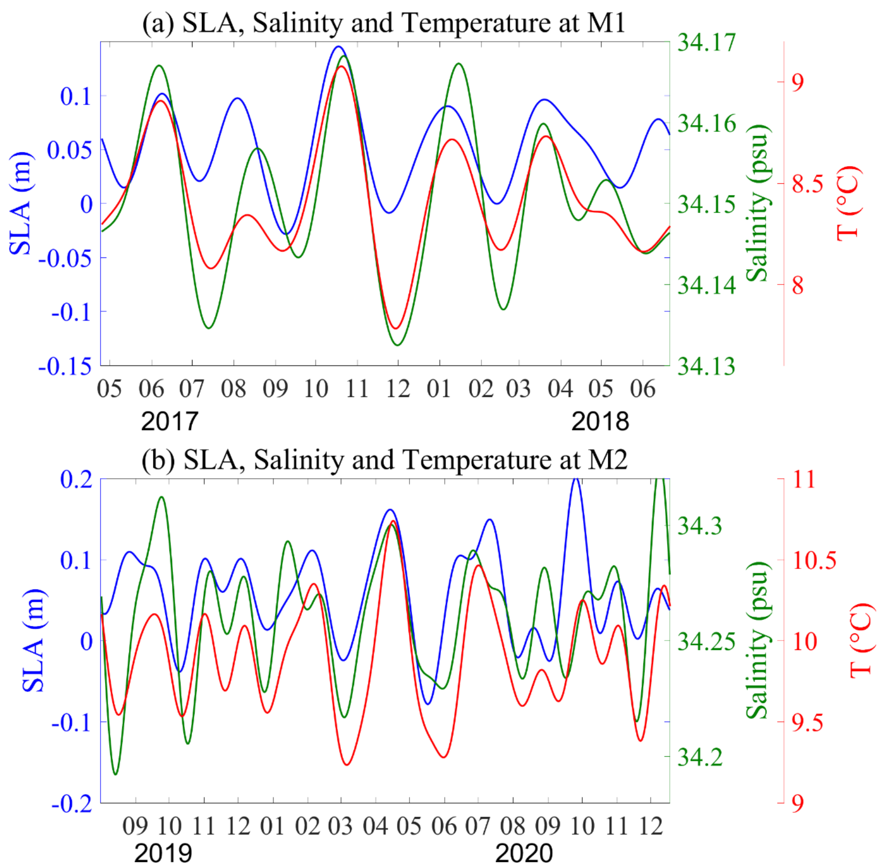

https://doi.org/10.5194/egusphere-2024-3227
Preprint. Discussion started: 21 October 2024

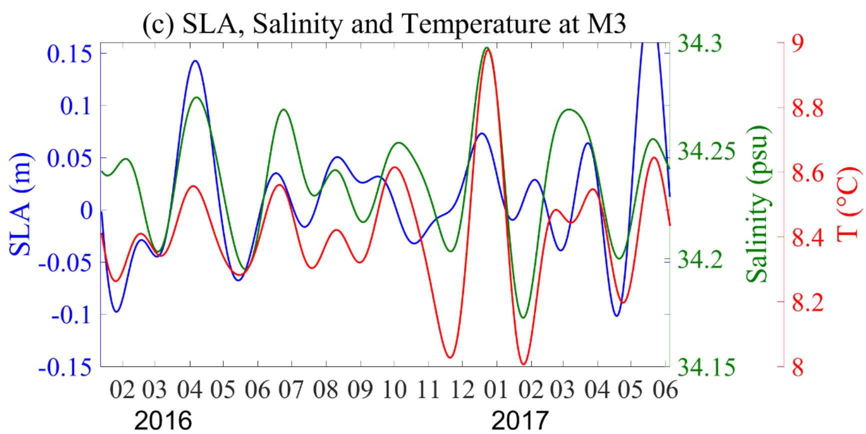

Figure 6. (a) The 20-100 day bandpass filtered time series of SLAs (blue curve), averaged temperature (red curve) and salinity from 500-800 m (green curve) at M1. (b) and (c) same as (a), but for M2 and M3.

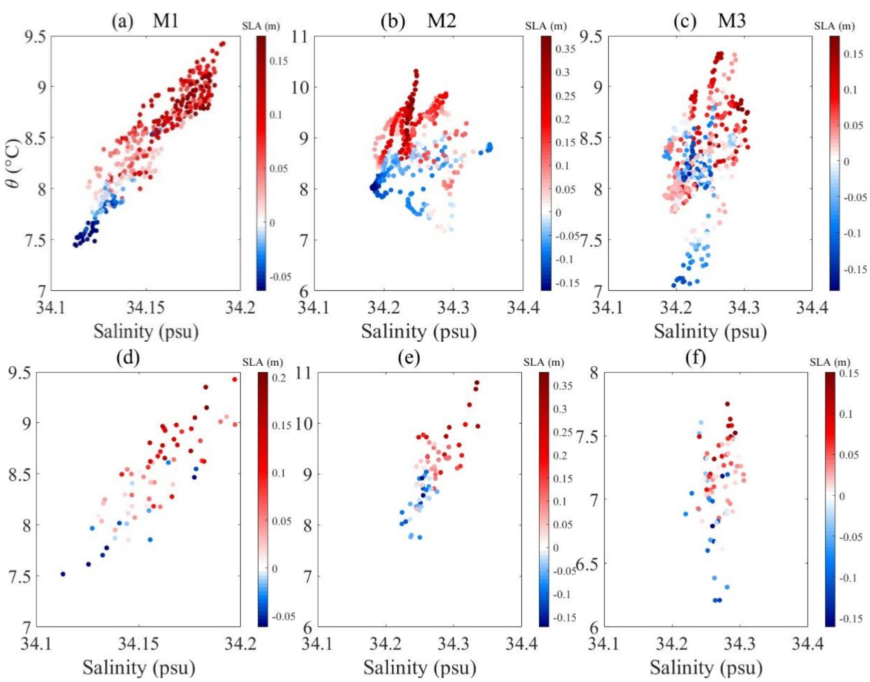

Figure 7. (a) The salinity and temperature data are shown a T-S scatter diagram at M1 where the color indicates SLAs. (b) and (c) are same as (a), but for M2 and M3. (d), (e) and (f) are T-S plots of 500-800 m averaged temperature and salinity data from CMEMS product in the intermediate layer corresponding to the locations of M1, M2, and M3, respectively.

https://doi.org/10.5194/egusphere-2024-3227
Preprint. Discussion started: 21 October 2024

The ISV of NPIW induced by mesoscale eddies

The presence of an ~80-day intraseasonal signals in the SLA that is consistent across moorings M1 to M3, along with its positive correlation, indicates that surface signals can significantly influence water mass changes at depths up to nearly 800 m in the ocean. To investigate the origin of the SLA signal, we analyzed the propagation of SLA over time along section at the same latitude as the moorings during the observation period. The SLA variations for observation periods M1, M2, and M3 are depicted in Fig. 8a, 8c and 8e, respectively, revealing westward-propagating alternating positive and negative band-shaped signals consistent with mesoscale eddy characteristics. To more precisely examine the link between the mesoscale eddies and variations in salinity of intermediate layer, we analyzed the longitude-time lag correlations between them as depicted in Fig. 8b, 8d and 8f. The correlation coefficients at all three locations reveal significant band-shaped patterns, with variations periods approximately between 60 to 80 days. The highest correlation coefficients recorded were 0.61, 0.5 and 0.6 for M1, M2 and M3, respectively. These findings indicate that the intraseasonal variability of temperature and salinity within the intermediate layer are closely associated with the westward propagation of mesoscale eddies. Considering existing research that has shown the impact of mesoscale eddies can reach depths beyond 1000 m (Zhang et al., 2015; Thoppil et al., 2011; Zhang et al., 2016; Zhang et al., 2015; George et al., 2021; Waite et al., 2016; Hausmann et al., 2017), it can be inferred that the periodic changes in water masses above 800 m observed at the three different mooring locations and times in this study are significantly influenced by mesoscale eddies.

The above studies were based on analyses across entire time series, below we conduct some case analyses by selecting moments of significant changes of temperature and salinity at intermediate layer, also that is characterized by large positive or negative anomalies of salinity, to investigate the presence of mesoscale eddies at the sea surface. At the M1 mooring site, we identified two moments Event 1 and Event 2 corresponding to higher salinity and lower salinity events, where time of Event 1 and Event 2 is October 15, 2017 in Fig. 6a and November 29, 2017 in Fig. 6a, respectively. Then the SLAs and current field distributions are extracted for these moments shown in Fig. 9a and 9b. Notably, during the high salinity event, an anticyclonic eddy was present at the sea surface above the observation site, while during the low salinity event, the SLA and current field exhibited characteristics of a cyclonic eddy. More consistently, a similar phenomenon is observed at the positions of the M2 and M3 distributed along the western boundary, shown in Fig. 9c to Fig. 9f. The changes in temperature and salinity at intermediate water observed by these moorings, distributed at different times and locations can be combined with the oceanographic process of mesoscale eddies. And at least at the moments of high variability there is a relationship between the increase in temperature and salinity caused by anticyclonic eddies and the decrease in temperature and salinity caused by cyclonic eddies.

https://doi.org/10.5194/egusphere-2024-3227
Preprint. Discussion started: 21 October 2024

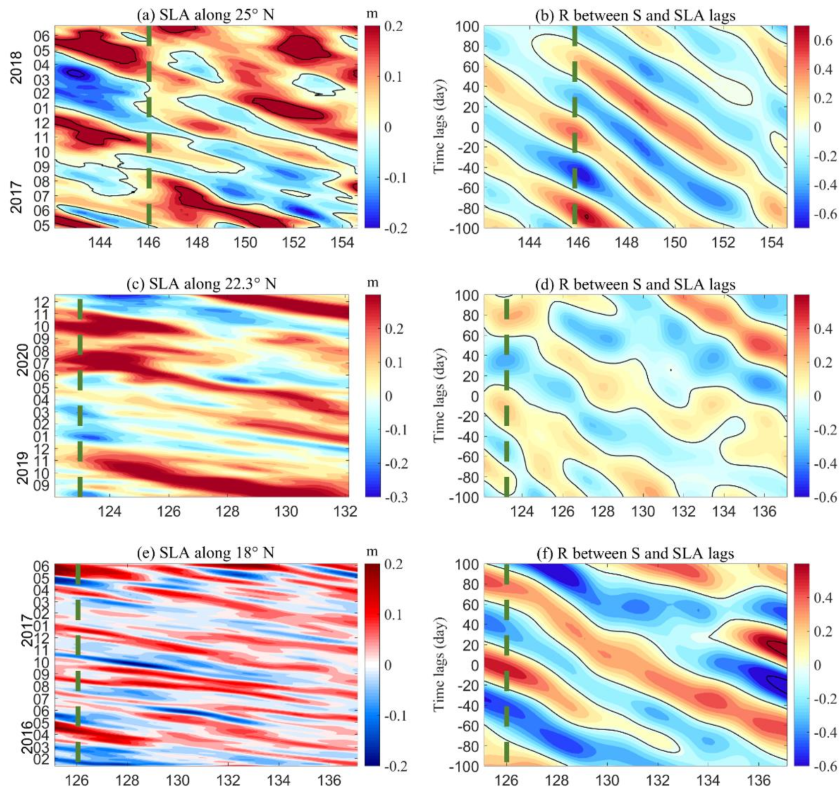

Figure 8. (a) The longitude-time contours of the SLAs along 25 °N; (b) The correlation coefficient between salinity at M1 and SLA at different time lags, the vertical coordinates -100 to 100 days in (b) represent SLA lagging salinity for 100 days and SLA exceeding salinity for 100 days, respectively. (c) and (e) are same as (a), but its along 22.3°N and 18°N, respectively. (d) and (f) are same as (b), but for salinity from M2 and M3, respectively. The black contours indicate the zero-line values. The green dash line represent the location of M1, M2 and M3, respectively.

https://doi.org/10.5194/egusphere-2024-3227
Preprint. Discussion started: 21 October 2024

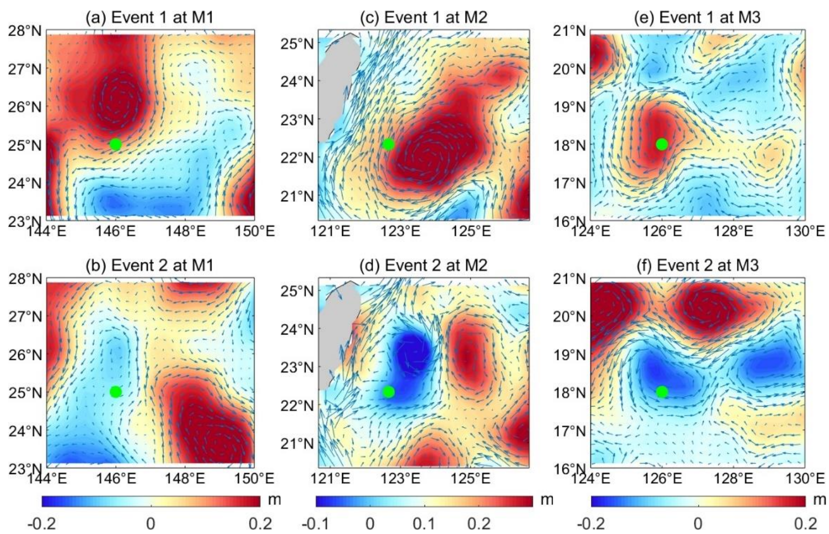

Figure 9. (a) and (b) are selected SLAs and surface geostrophic current maps corresponding to the moments of high salinity (Event 1) and low salinity (Event 2) observed from M1, respectively, where time of Event 1 corresponds to October 15, 2017 in Fig. 6a, and Event 2 corresponds to November 29, 2017 in Fig. 6a. (c) and (d) are same as (a) and (b), but for mooring site M2, where time of Event 1 and Event 2 at M2 corresponding to April 20, 2020 and March 5, 2020 showed in Fig. 6b. (e) and (f) are same as (a) and (b), but for mooring site M3, where time of Event 1 and Event 2 at M3 corresponding to April 10, 2016 and April 15, 2017 showed in Fig. 6c. The green dots denotes the mooring site, the colors shading represent the SLAs and the arrows indicate the surface geostrophic current.

The mechanism of NPIW variations influenced by mesoscale eddies

Direct observations from moorings are undoubtedly the most effective method for research. Although the variations in temperature and salinity at several moorings are correlated with mesoscale eddies, it is challenging to understand from a broader perspective how mesoscale eddies influence intermediate layer temperature and salinity changes in different regions. Therefore, we turned to reanalysis data to analyze the mechanisms by which mesoscale eddies affect NPIW. We selected temperature, salinity, and current field data from the Copernicus Marine Environment Monitoring Service (CMEMS) product, which has been described in detail in the Data and Methods section. To ensure a rigorous analysis, we need to make a reasonableness judgment about the data selected. Power spectral analyses were performed on the reanalysis data for the same observation periods at the locations of the three moorings to verify the presence of intraseasonal signals. The results well presented in Fig. 10 showed ~60-80 days intraseasonal cycles in salinity at intermediate layer at all three locations, also this result

https://doi.org/10.5194/egusphere-2024-3227
Preprint. Discussion started: 21 October 2024

generally consistent with mooring observations. Next, we compared scatter plots of temperature and salinity with SLA, with the results displayed in Fig. 7d, Fig. 7e and Fig. 7f, corresponding to observations from moorings M1, M2, and M3 in Fig. 7a, Fig. 7b and Fig. 7c, respectively. From these figures, we identified a consistent pattern from CMEMS product data with the mooring observations: higher temperatures and salinities were associated with positive SLA, and lower temperatures and salinities corresponded to negative SLA. Thus, the intermediate layer temperature and salinity characteristics from the reanalysis data showed results consistent with observations. As this paper is a qualitative analysis of the relationship between temperature and salinity variations and mesoscale eddies, these features obtained from reanalyzing data that are consistent with the real measurements can be used in the discussion that follows.

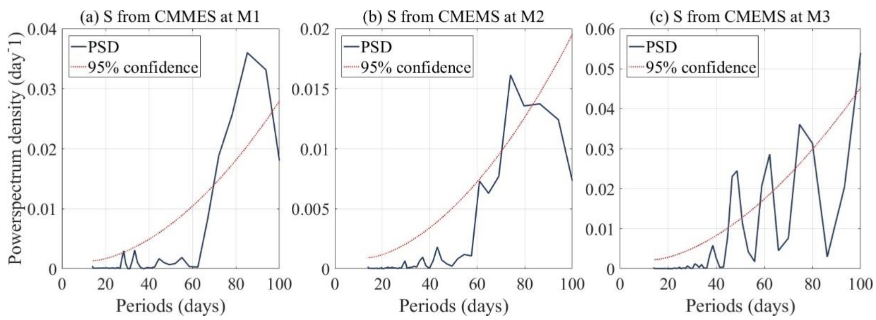

Figure 10. (a) The power spectrum density of 500-800 m averaged salinity at location of M1 from CMEMS data. (b) and (c) are same as (a), but for location of M2 and M3, respectively. The red dash line represent the 95% confidence level.

This study concentrates on the observation of low and high salinity events in the intermediate layer at mooring M1, also prior analyses have identified an intraseasonal signal with inverse phase characteristics at a depth of 700 m, as shown in Fig. 5. Consequently, reanalysis data was employed to calculate the averages of the current field and salinity distribution at depths ranging from 500 to 700 m and 700 to 900 m, with results displayed in Fig. 11a to 11d. The composite current field distribution clearly shows the presence of typical anticyclonic and cyclonic eddies during high salinity and low salinity events, respectively. In high salinity events, anticyclonic eddies were found to cause an increase in salinity (and correspondingly temperature increase) in the 500 m to700 m (Fig. 11a), while inducing lower salinity in the 700 to 900 m layer (Fig. 11c). This suggests that around the core depth of the intermediate water, anticyclonic eddies lead to increased salinity above it and lower salinity below it. During low salinity events showed in Fig. 11b and 11d, the significant presence of cyclonic eddies results in lower salinity characteristics at 500-700 m and relatively higher salinity at 700-900 m. Fig. 11 also shows that even away from the mooring points, nearby anticyclonic and cyclonic eddies cause similar characteristics. These distinct salinity changes during anticyclonic (cyclonic) eddy periods are related to the eddies' internal vertical transport.

https://doi.org/10.5194/egusphere-2024-3227
Preprint. Discussion started: 21 October 2024

In the North Pacific region, the salinity profile structure is inversely *S*-shaped, with two peaks indicating high salinity features in the subsurface layer and low salinity in the intermediate layer. Thus, when anticyclonic eddies occur, the downward movement of water masses within the eddy causes subsurface high temperature and high salinity water to mix into the intermediate layer, leading to increased temperature and salinity at intermediate layer. Similarly, this downward movement causes low salinity intermediate layer water to mix downwards, resulting in relatively lower temperature and salinity characteristics in the deeper layer. Conversely, when cyclonic eddies occur, their internal upward movement causes low salinity water at intermediate layer to mix upwards, resulting in low temperature and salinity characteristics above the intermediate layer, while the upward mixing of deeper high salinity water masses leads to increased temperature and salinity anomalies in the intermediate layer. These phenomena demonstrate how the eddies' internal relative movements can alter local temperature and salinity, causing thermohaline mixing.

For the observations near the western boundary at moorings M2 and M3, it is not only the anomalies in temperature and salinity caused by the internal movements of mesoscale eddies impact the intermediate water masses. Moreover, due to the relatively complex surrounding water mass structure, the variations might differ from those at M1. Near M2 mooring location, existing studies have indicated the influence of South China Sea Intermediate Water (SCSIW) and Kuroshio Intermediate Water (KIW), with Mensah et al., (2015) and Ren et al. (2022) providing a detailed analysis of the factors affecting intermediate water changes at this location using servals cruise observation data and nearby mooring data. Revisiting Fig. 12, we observe significant differences in salinity caused by anticyclonic and cyclonic eddies. During anticyclonic eddies, higher salinity SCSIW may flow out of the Luzon Strait under the influence of mesoscale eddies, leading to increased intermediate layer salinity east of Taiwan. Conversely, under cyclonic eddies, it seems less likely for SCSIW to flow out to the western pacific through the Luzon Strait, resulting in relatively lower salinity. For M3 mooring location, located at the southwestern edge of the NPIW distribution in the entire North Pacific (Fig. 1a), the water masses to the south have relatively higher salinity. Therefore, during anticyclonic eddy events, it appears that anticyclonic eddies can draw higher salinity water masses from the south into northern positions (Fig. 13a), while during cyclonic eddy events, the opposite occurs, with cyclonic eddies seemingly pushing relatively lower salinity water masses southward (Fig. 13b). Wang et al. (2016) also demonstrated at 8°N that eddies can act as mixers when there are differences in water mass characteristics between the Northern and Southern Hemispheres. Although M3 mooring location is further north than that studied by Wang et al., (2016), the mechanism appears to share similar characteristics to some extent.

With the above analysis, despite the inconsistencies in the depth and characteristics of the intermediate water masses, or the complexity and variability of certain localized water masses, we find the property that anticyclonic eddies lead to higher temperatures and salinities in the NPIW, while cyclonic eddies lead to lower temperatures and salinities in the NPIW. Given the prevalence of mesoscale eddies in the ocean, this continuous stirring process by mesoscale eddies enhances thermohaline mixing and

https://doi.org/10.5194/egusphere-2024-3227
Preprint. Discussion started: 21 October 2024

energy exchange in the upper layers of the ocean.

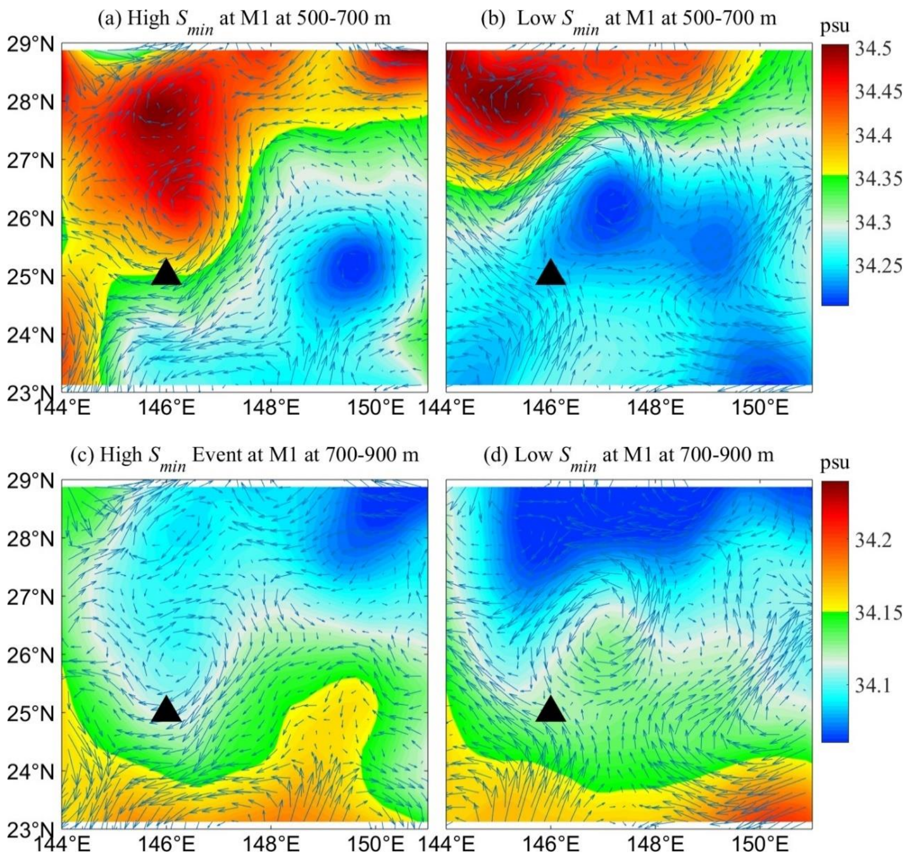

Figure 11. (a) Composite map of salinity (colors) and current (blue arrows) averaged between 500 to 700 m at high salinity event around the M1. (b) Composite map of salinity (colors) and current (blue arrows) averaged between 500 m to 700 m at low salinity event. (c) same as (a), but for 700 m to 900 m at high salinity event. (d) same as (c), but for low salinity event. The black triangle is the mooring site.

https://doi.org/10.5194/egusphere-2024-3227
Preprint. Discussion started: 21 October 2024

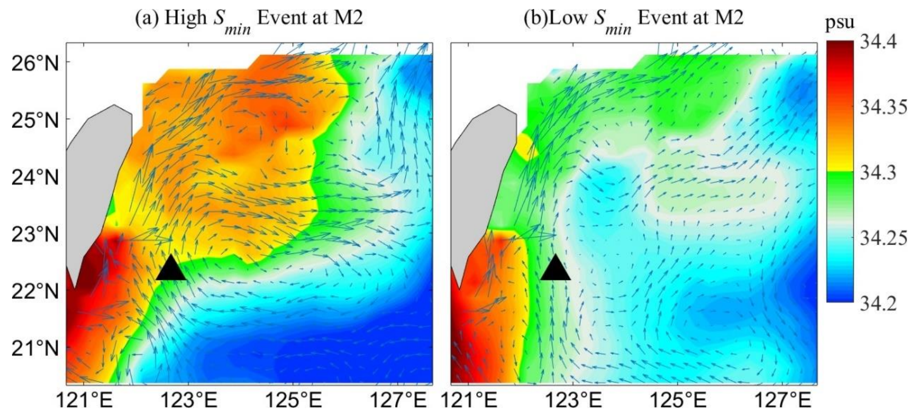

Figure 12. (a) Composite map of salinity (colors) and current (blue arrows) averaged between 500 to 700 m at high salinity event around M2. (b) Composite map of salinity (colors) and current (blue arrows) averaged between 500 m to 700 m at low salinity event around M2. The black triangle is the mooring site M2.

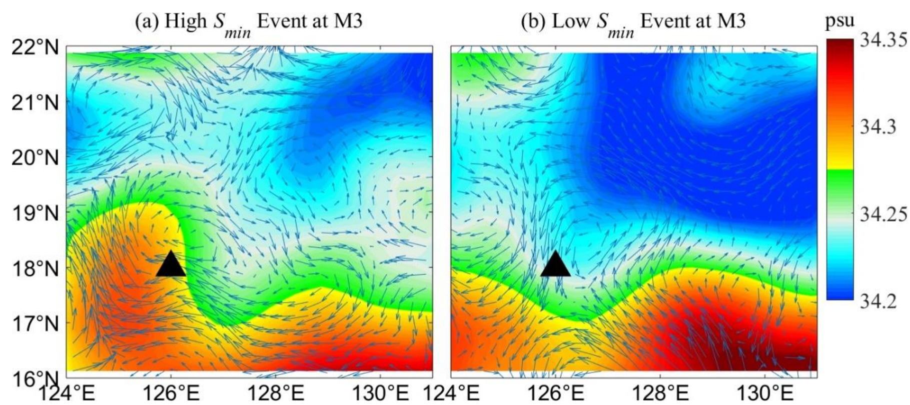

Figure 13. (a) Composite map of salinity (colors) and current (blue arrows) averaged between 500 to 700 m at high salinity event around M3. (b) Composite map of salinity (colors) and current (blue arrows) averaged between 500 m to 700 m at low salinity event around M3. The black triangle is the mooring site M3.

Conclusion

In this study, we conducted direct observations of the temperature and salinity of the North Pacific Intermediate Water (NPIW) over a period exceeding 14 months using three moorings deployed at different locations and measuring times in the North Pacific. The observations revealed that the core low salinity depths of NPIW at locations M1, M2, and M3 are approximately 700m, 600m, and 550m, respectively. The lowest salinity minima observed was around 34.15 psu at M1, with M2 having slightly higher salinity and M3 the highest. It was also noted that the intermediate water near the western boundary at location M2 exhibited a larger range of variation between 34.1 psu to 34.35 psu, and the isopycnal depths at $26.8\sigma_\theta$ varied by more than 100 meters. While the intermediate water at M1 having a deeper depth, showed relatively minor variations of minimum salinity. Wavelet analysis revealed that NPIW exhibits a consistent intraseasonal variability characteristic, with the cycles at locations M1, M2, and M3 estimated to be approximately 60~80 days.

By analyzing data from the AVISO satellite altimetry, we have discerned that the intraseasonal variations of the NPIW are attributable to the westward propagating of mesoscale eddies. This conclusion is supported by the computation of correlation coefficients between SLA and intermediate layer salinity at three distinct locations, designated M1, M2, and M3, which yielded values of 0.61, 0.5, and 0.6, respectively. These findings suggest a significant relationship between SLA and salinity variations in these regions. Further by case studies, we have elucidated the influence of mesoscale eddies on the thermohaline properties of the intermediate layer. Specifically, during the occurrence of anticyclonic eddy events, the NPIW exhibits characterized of higher temperature and salinity, whereas cyclonic eddy periods are associated with a decrease in both temperature and salinity in the NPIW.

Simultaneously, global observational three-dimensional temperature and salinity data products were employed to analyze the mechanisms by which mesoscale eddies induce changes in NPIW. Due to the variability in background circulation characteristics and water mass properties across different regions, the mechanisms of variation of NPIW at the locations of the three moorings exhibit some differences. At the M1 location, an inverse phase change in temperature and salinity occurs above and below a depth of 700 m. The appearance of anticyclonic eddies induces downward transport, leading to positive anomalies in temperature and salinity in the intermediate layer due to the downward movement of higher salinity of subsurface waters, while the downward movement of lower salinity intermediate layer waters results in negative anomalies below 700m. At the M2 location, influenced by the Kuroshio, mesoscale eddies, SCSIW and KIW, temperature and salinity changes are not only affected by the vertical movement within eddies but may also be influenced by the outflow of SCSIW through the Luzon Strait, as suggested by Mensah et al. (2015) and Ren et al. (2022). Their research found that anticyclonic (cyclonic) eddies could enhance (weaken) the Kuroshio and increase (reduce) the passage of SCSIW through the Luzon Strait, resulting in relatively higher (lower) temperature and salinity changes near the M2 location. At M3, located at the edge of the NPIW distribution based on the 26.8 isopycnal distribution, the region is characterized by relatively higher salinity intermediate water masses to its south. Thus during anticyclonic eddies, higher salinity southern water masses are drawn into the northern positions, while during cyclonic eddies, relatively lower salinity northern intermediate water masses are pushed southward. Also the result found that under the influence of the eddy, the change in salinity in the intermediate layer can reach to 0.3 psu, and the depth of the low-salt core

https://doi.org/10.5194/egusphere-2024-3227
Preprint. Discussion started: 21 October 2024

can vary by hundreds of meters.

Therefore, NPIW demonstrates consistent intraseasonal variability across a range of latitudes and spatiotemporal scales. This consistency is largely attributed to the NPIW's location within zones frequently impacted by mesoscale eddies. These dynamic features exert a continuous influence on the NPIW, modulating its properties and behavior. Given the pivotal role of mesoscale eddies in shaping the characteristics of intermediate waters, future research should prioritize the investigation of their contributions to heat and energy fluxes within the ocean's intermediate layer. Such studies are crucial for understanding the mechanisms underlying the NPIW's formation and evolution, particularly in the context of ongoing climate change. Furthermore, elucidating the interactions between the NPIW and the global carbon cycle will enhance our comprehension of its significance within the marine carbon budget. Additionally, exploring the NPIW's influence on marine ecosystems will provide valuable insights into its ecological role, offering a more holistic understanding of its importance in the broader context of oceanography and climate science.

Competing Interests Statement: The authors have no conflicts of interest to declare.

Acknowledgments

This work is supported by the National Natural Science Foundation of China (No. 42206032), and the Natural Science Foundation of Shandong Province (No. ZR2022QD045). We would like to thank all the personnel of the R/V Science for their contribution to the data acquisition.

Data Availability Statement

The mooring data are from Oceanographic Data Center, Chinese Academy of Sciences(CASODC), and the website: http://english.casodc.com/data/metadata-special-detail?id=1769562089216626690. The WOA data are available from website: https://www.ncei.noaa.gov/products/world-ocean-atlas. The merged gridded altimetry data can be downloaded from the website: https://data.marine.copernicus.eu/. The Multi Observation Global Ocean data can be downloaded from the website: https://data.marine.copernicus.eu/.

Reference

Auad, G., Kennett, J., & Miller, A. (2003). North Pacific Intermediate Water response to a modern climate warming shift. *Journal of Geophysical Research*, **108**(C11),3349. DOI: 10.1029/2003JC001987.

Bingham F, Lukas R. (1994). The southward intrusion of North Pacific Intermediate Water along the

https://doi.org/10.5194/egusphere-2024-3227
Preprint. Discussion started: 21 October 2024

Mindanao coast. *Journal of Physical Oceanography*, **24**:141–154.

Bingham, F. M. , & Lukas, R. . (1995). The distribution of intermediate water in the western equatorial pacific during January–February 1986. *Deep Sea Research Part I Oceanographic Research Papers*, **42**(9), 1545-1573.

Bingham, F. M., & Lukas, R. (1996). Seasonal cycles of temperature, salinity and dissolved oxygen observed in the Hawaii Ocean Time-series. *Deep-Sea Research Part II: Topical Studies in Oceanography*, **43**(2-3), 199-213.

Boyer, T.P., Antonov, J.I., Baranova, O.K., Coleman, C., Garcia, H.E., Grodsky, A., Johnson, D.R. Locarnini, R.A., Mishonov, A.V., O'Brien,T.D., Paver, C.R., Reagan,J.R., Seidov, D., Smolyar, I.V. and Zweng, M.M. (2013) World Ocean Database 2013. Silver Spring, MD, National Oceanographic Data Center, 208pp. (NOAA Atlas NESDIS, 72).

Busecke, J.J., & Abernathey, R.P. (2019). Ocean mesoscale mixing linked to climate variability. *Science Advances, **5***.

Chaigneau, A., Eldin, G., & Dewitte, B. (2009). Eddy activity in the four major upwelling systems from satellite altimetry (1992-2007). *Progress in Oceanography, **83***, 117-123.

Chaigneau, A., Gizolme, A., & Grados, C. (2008). Mesoscale eddies off Peru in altimeter records: Identification algorithms and eddy spatio-temporal patterns. *Progress in Oceanography, **79***, 106-119.

Chelton, D. Mesoscale eddy effects. *Nature Geoscience*. **6**, 594-595 (2013).

Chelton, D., Gaube, P., Schlax, M.G., Early, J.J., & Samelson, R.M. (2011). The Influence of Nonlinear Mesoscale Eddies on Near-Surface Oceanic Chlorophyll. *Science, **334***, 328 - 332.

Chelton, D., Schlax, M.G., & Samelson, R.M. (2011). Global observations of nonlinear mesoscale eddies. *Progress in Oceanography, **91***, 167-216.

Chelton, D., Schlax, M.G., Samelson, R.M., & de Szoeke, R.A. (2007). Global observations of large oceanic eddies. *Geophysical Research Letters, **34***.

Dong, C., McWilliams, J. C., Liu, Y. & Chen, D. (2014). Global heat and salt transports by eddy movement. *Nature Communications*. **5**, 3294 (2014).

Frenger, I., Gruber, N., Knutti, R., & Münnich, M. (2013). Imprint of Southern Ocean eddies on winds, clouds and rainfall. *Nature Geoscience, **6***, 608-612.

Fujii, Y., Nakano, T., Usui, N., Matsumoto, S., Tsujino, H., & Kamachi, M. (2013). Pathways of the North Pacific Intermediate Water identified through the tangent linear and adjoint models of an ocean general circulation model. *Journal of Geophysical Research*, **118**, 2035-2051.

George, T. M., Manucharyan, G., & Thompson, A. F. (2021). Deep learning to infer eddy heat fluxes from sea surface height patterns of mesoscale turbulence. *Nature Communications*, **12**, 800. DOI: 10.1038/s41467-020-20779-9.

Gordon AL, Fine RA. (1996). Pathways of the water between the Pacific and Indian Oceans in the Indonesian seas. *Nature* **379**:146–149.

Hansell, D. A., Carlson, C., & Suzuki, Y. (2002). Dissolved organic carbon export with North Pacific Intermediate Water formation. *Global Biogeochemical Cycles*, **16**(1). DOI: 10.1029/2000GB001361.

Hausmann, U., McGillicuddy, D., & Marshall, J. (2017). Observed mesoscale eddy signatures in Southern Ocean surface mixed-layer depth. *Journal of Geophysical Research, **122***, 617-635. DOI: 10.1002/2016jc012225.

Kashino Y, Aoyama M, Kawano T, Hendiarti N, Syaefudin Anantasena Y, Muneyama K, Watanabe H .

https://doi.org/10.5194/egusphere-2024-3227
Preprint. Discussion started: 21 October 2024

(1996). The water masses between Mindanao and New Guinea. *Journal of Geophysical Research,* **101**(C5):12391–12400.

Kashino Y, Watanabe H, Herunadi H, Aoyama M, Hartoyo D (1999).Current variability at the Pacific entrance of the Indonesian throughflow. *Journal of Geophysical Research*, 104(C5):11021–11035.

Kouketsu, S., I. Kaneko, T. Kawano, H. Uchida, T. Doi, and M. Fukasawa (2007), Changes of North Pacific Intermediate Water properties in the subtropical gyre, *Geophysical Research Letters*, **34**(2), L02605, doi:10.1029/2006GL028499.

Martínez‐Moreno, J., Hogg, A.M., England, M.H., Constantinou, N.C., Kiss, A.E., & Morrison, A.K. (2020). Global changes in oceanic mesoscale currents over the satellite altimetry record. *Nature Climate Change, **11***, 397 - 403.

Masuda, S. , Awaji, T. , Sugiura, N. , Ishikawa, Y. , Baba, K. , & Horiuchi, K. , et al. (2003). Improved estimates of the dynamical state of the north pacific ocean from a 4 dimensional variational data assimilation. *Geophysical Research Letters*, **30**(16).

Masujima, M., & Yasuda, I. (2009). Distribution and Modification of North Pacific Intermediate Water around the Subarctic Frontal Zone East of 150°E. *Journal of Physical Oceanography, **39***, 1462-1474.

Mensah, V., Jan, S., Chang, M., & Yang, Y. (2015). Intraseasonal to seasonal variability of the intermediate waters along the Kuroshio path east of Taiwan. *Journal of Geophysical Research*, **120**, 5473-5489. https://doi.org/10.1002/2015JC010768.

Meredith, M.P., Garabato, A.N., Hogg, A.M., & Farneti, R. (2011). Sensitivity of the Overturning Circulation in the Southern Ocean to Decadal Changes in Wind Forcing. *Journal of Climate,* **25**, 99-110.

Nakano, T., Kaneko, I., Endoh, M., & Kamachi, M. (2005). Interannual and Decadal Variabilities of NPIW Salinity Minimum Core Observed along JMA's Hydrographic Repeat Sections. *Journal of Oceanography*, **61**, 681-697.

Nakanowatari, T., Mitsudera, H., Motoi, T., Ishikawa, I., Ohshima, K.I., & Wakatsuchi, M. (2015). Multidecadal-Scale Freshening at the Salinity Minimum in the Western Part of North Pacific: Importance of Wind-Driven Cross-Gyre Transport of Subarctic Water to the Subtropical Gyre. *Journal of Physical Oceanography,* **45**, 988-1008.

Nishioka, J., Obata, H., Ogawa, H., Ono, K., Yamashita, Y., Lee, K., Takeda, S., & Yasuda, I. (2020). Subpolar marginal seas fuel the North Pacific through the intermediate water at the termination of the global ocean circulation. *Proceedings of the National Academy of Sciences of the United States of America*, **117**(24), 12665-12673. DOI: 10.1073/pnas.2000658117.

Ohkushi, K., Itaki, T., & Nemoto, N. (2003). Last Glacial–Holocene change in intermediate-water ventilation in the Northwestern Pacific. *Quaternary Science Reviews*, **22**(14), 1477-1484. DOI: 10.1016/S0277-3791(03)00082-9.

Ohshima, K., Nakanowatari, T., Riser, S., & Wakatsuchi, M. (2010). Seasonal variation in the in and outflow of the Okhotsk Sea with the North Pacific. *Deep-Sea Research Part II: Topical Studies in Oceanography*, **57**(13-14), 1247-1256.

Oka, E., Katsura, S., Inoue, H., Kojima, A., Kitamoto, M., Nakano, T., & Suga, T. (2017). Long-term change and variation of salinity in the western North Pacific subtropical gyre revealed by 50-year long observations along 137°E. *Journal of Oceanography*, **73**, 479-490. DOI: 10.1007/s10872-017-0416-2

Qiu, B. (1995). Why Is the Spreading of the North Pacific Intermediate Water Confined on Density

https://doi.org/10.5194/egusphere-2024-3227
Preprint. Discussion started: 21 October 2024

Surfaces around σθ = 26.8?. *Journal of Physical Oceanography*, **25**(1), 168-180.

Qiu, B., & Chen, S. (2005). Eddy-Induced Heat Transport in the Subtropical North Pacific from Argo, TMI, and Altimetry Measurements. *Journal of Physical Oceanography*, **35**(4), 458-473.

Qiu, B., & Chen, S. (2011). Effect of Decadal Kuroshio Extension Jet and Eddy Variability on the Modification of North Pacific Intermediate Water. *Journal of Physical Oceanography*, **41**(3), 503-515.

Ren, Q., Yu, F., Nan, F. et al. Effects of mesoscale eddies on intraseasonal variability of intermediate water east of Taiwan. *Scientifc Reports*, **12**, 9182 (2022). https://doi.org/10.1038/s41598-022-13274-2

Richardson, P.L. (1983). Eddy kinetic energy in the North Atlantic from surface drifters. *Journal of Geophysical Research,* **88**, 4355-4367.

Robinson, A.R., & Leslie, W.G. (1985). Estimation and prediction of oceanic Eddy fields. *Progress in Oceanography,* **14**, 485-510.

Solomon, A., McCreary, J., Kleeman, R., & Klinger, B. A. (2003). Interannual and Decadal Variability in an Intermediate Coupled Model of the Pacific Region. *Journal of Climate*, **16**, 383-405.

Talley, L. D. , & Yun, J. Y. . (2001). The role of cabbeling and double diffusion in setting the density of the north pacific intermediate water salinity minimum. *Journal of Physical Oceanography*. **31**(6), 1538-1549.

Talley, L.D. (1993). Distribution and formation of North Pacific Intermediate Water. *Journal of Physical Oceanography,* **23**(3), 517-537.

Talley, L.D., Nagata, Y., Fujimura, M., Iwao, T., Kono, T., Inagake, D., Hirai, M., & Okuda, K. (1995). North Pacific Intermediate Water in the Kuroshio/Oyashio Mixed Water Region. *Journal of Physical Oceanography,* **25**, 475-501.

Thoppil, P., Richman, J., & Hogan, P. (2011). Energetics of a global ocean circulation model compared to observations. *Geophysical Research Letters, **38**(15),* L15607.

Tsunogai, S. (2002). The Western North Pacific Playing a Key Role in Global Biogeochemical Fluxes. *Journal of Oceanography*, **58**(2), 245-257. DOI: 10.1023/A:1015805607724.

Ueno, H., & Yasuda, I. (2004). Intermediate water circulation in the North Pacific subarctic and northern subtropical regions. *Journal of Geophysical Research*, 108, 3348.

Waite, A., Stemmann, L., Guidi, L., Calil, P., Hogg, A., Feng, M., Thompson, P., Picheral, M., & Gorsky, G. (2016). The wineglass effect shapes particle export to the deep ocean in mesoscale eddies. *Geophysical Research Letters,* **43**, 9791-9800. DOI: 10.1002/2015GL066463.

Wang, F., Song, L., Li, Y., Liu, C., Wang, J., Lin, P., Yang, G., Zhao, J., Diao, X., Zhang, D., & Hu, D. (2016). Semiannually alternating exchange of intermediate waters east of the Philippines. *Geophysical Research Letters*, **43**, 7059-7065. DOI: 10.1002/2016GL069323

Wong, A., Bindoff, N. & Church, J. (1999). Large-scale freshening of intermediate waters in the Pacific and Indian oceans. *Nature* **400**, 440–443.

Wunsch, C & Ferrari, R. (2004). Vertical mixing, energy, and the general circulation of the oceans. *Annual Review of Fluid Mechanics*. **36**, 281-314.

Wunsch, C. (2007), The past and future ocean circulation from a contemporary perspective, in Ocean Circulation: Mechanisms and Impacts-Past and Future Changes of Meridional Overturning, Geophys. Monogr. Ser., vol. 173, pp. 53–74, AGU, Washington, D. C.

Wyrtki, K., Magaard, L., & Hager, J.G. (1976). Eddy energy in the oceans. *Journal of Geophysical Research,* **81**, 2641-2646.

https://doi.org/10.5194/egusphere-2024-3227
Preprint. Discussion started: 21 October 2024

Yasuda, I. (1997). The origin of the North Pacific Intermediate Water. *Journal of Geophysical Research: Oceans*, **102**(C1), 893-909.

Yasuda, I. . (2004). North pacific intermediate water: progress in sage (subarctic gyre experiment) and related projects. *Journal of Oceanography*, **60**(2), 385-395.

You, Y. (2003). The pathway and circulation of North Pacific Intermediate Water. *Geophysical Research Letters,* **30***, 2291*.

Van Scoy, K. A., and E. R. M. Druffel (1993), Ventilation and transport of thermocline and intermediate waters in the northeast Pacific during recent El Niños, *Journal of Geophysical Research: Oceans*, **98**(C10), 18083–18088.

Zhang, W., Xue, H., Chai, F., & Ni, Q. (2015). Dynamical processes within an anticyclonic eddy revealed from Argo floats. *Geophysical Research Letters,* **42**, 2342-2350. DOI: 10.1002/2015GL063120.

Zhang, Y., Liu, Z., Zhao, Y., Li, J., & Liang, X. (2015). Effect of surface mesoscale eddies on deep-sea currents and mixing in the northeastern South China Sea. *Deep-sea Research Part II: Topical Studies in Oceanography,* **122**, 6-14. DOI: 10.1016/J.DSR2.2015.07.007.

Zhang, Z., Tian, J., Qiu, B., Zhao, W., Chang, P., Wu, D., & Wan, X. (2016). Observed 3D Structure, Generation, and Dissipation of Oceanic Mesoscale Eddies in the South China Sea. *Scientific Reports,* **6***,* 24349 . DOI: 10.1038/srep24349.

Zhang, Z., Wang, W., & Qiu, B. (2014). Oceanic mass transport by mesoscale eddies. *Science,* **345**, 322 - 324.